RSC Advances

Accepted Manuscript

This article can be cited before page numbers have been issued, to do this please use: Z. Li, J. Torgersen, A. Ajami, S. Mühleder, X. Qin, W. Husinsky, W. Holnthoner, A. Ovsianikov, J. Stampfl and R. Liska, *RSC Adv.*, 2013, DOI: 10.1039/C3RA42918K.

RSC Advances

Dynamic Article Links ►

View Article Online
DOI: 10.1039/C3RA42918K

Cite this: DOI: 10.1039/c0xx00000x

www.rsc.org/xxxxxx

ARTICLE TYPE

Initiation Efficiency and Cytotoxicity of Novel Water-soluble Two-photon Photoinitiators for Direct 3D Microfabrication of Hydrogels

Zhiquan Li,[a,e] Jan Torgersen,[b,e] Aliasghar Ajami,[c] Severin Mühleder,[d,e] Xiaohua Qin,[a,e] Wolfgang Husinsky,[c] Wolfgang Holnthoner,[d,e] Aleksandr Ovsianikov,[b,e] Jürgen Stampfl,[b,e] Robert Liska[a,e]*

Received (in XXX, XXX) Xth XXXXXXXXX 20XX, Accepted Xth XXXXXXXXX 20XX
DOI: 10.1039/b000000x

The lack of efficient water-soluble two-photon absorption (TPA) photoinitiators has been a critical obstruction for three dimensional hydrogel microfabrications with high water load by two-photon induced polymerization (TPIP). In this paper, a series of cyclic benzylidene ketone-based two-photon initiators, containing carboxylic acid sodium salts to improve water solubility, were synthesized via classical aldol condensation reactions. Cytotoxicity of cyclopentanone-based photoinitiators is as low as that of the well-known biocompatible photoinitiator Irgacure 2959 as assessed in the dark with MG63 cell line. In z-scan measurement, the TPA cross sections of the investigated initiators are only moderate in water, while the TPA values for hydrophobic analogues measured in chloroform were much higher. All novel initiators exhibited broad processing windows in TPIP tests using hydrophilic photopolymers with up to 50 wt% of water. Impressively, microfabrication of hydrogels with excellent precision was possible at a writing speed as high as 100 mm/s.

INTRODUCTION

The precise microfabrication of hydrogels with arbitrary predesigned shapes has become critical for numerous biological applications such as the construction of biosensors[1] and the creation of soft scaffolds[2] for tissue engineering. Several solid free-form additive manufacturing techniques (laser-based, nozzle-based and printer-based) have been applied to hydrogel processing.[3] Among these microfabrication techniques, two-photon induced polymerization (TPIP) attracts considerable attention due to the unique capacity provided for direct 3D writing.[4] Since two-photon absorption can only occur within the small laser focal volume, excellent spatial control with high resolution in the sub-micrometer range can be obtained[5]. Moreover, the long wavelength of the excitation source offers the advantages of deeper tissue penetration with reduced risk for unintended photodamage[6], making TPIP especially suitable for various biological applications.[2, 7]

Generally, during the fabrication process, the photoactive resin, usually containing multifunctional acrylate-based monomers and a photoinitiator (PI), is cured within the focal point of the pulsed laser beam. Although TPIP has already shown great potentials in biofabrication with hydrogels,[8, 9] further development has been limited, primarily due to the lack of efficient two-photon absorption (TPA) initiation systems.[10, 11] Ideal TPA PIs for biofabrication should possess high initiation efficiency, sufficient hydrophilicity and good biocompatibility, or more specifically low cytotoxicity, which is critical when processing in the presence of cells. In the last decades, plenty of TPA active hydrophilic chromophores have been reported.[12, 13] However, nearly all of them are fluorescent dyes for bioimaging applications.[14, 15] Fluorescent dyes are however not optimal as polymerization initiators since initiation and fluorescence are essentially competitive relaxation pathways for excited state species. Originally, the commercial UV photoinitiator Irgacure 2959 was used for TPIP due to its reasonable hydrophilicity and low cytotoxicity.[16] However, this initiator is only processable with 515 nm pulsed laser light, which tends to increase the risk for denaturing surrounding proteins.[17] Another strategy developed to improve water solubility of commercially available, hydrophobic initiators is based on the assistance of nonionic surfactants.[11] Though this approach facilitates the fabrication of hydrogel structures within an aqueous formulation via TPIP, large amounts of surfactant are needed to ensure adequate initiation efficiency and cell lysis becomes a concern.

Until now, the most popular hydrophilic initiation system for TPIP is a dye-amine combination. Due to suitable absorption at desired wavelength and easy accessibility, commercial hydrophilic xanthene dyes, such as rose bengal, eosin and erythrosine, were applied in TPIP with amines as co-initiators.[18, 19] In this initiation system, the dye is excited by TPA and subsequently intermolecular electron transfer followed by hydrogen transfer from the amine to the excited dye generates active amine radicals to induce polymerization.[20, 21] The main drawbacks of such an initiation system are the requirements of high laser intensities (~100 mW) and long exposure times (300 - 400 μ s) due to the small TPA cross section of the dye.[22] Additionally, intrinsic limitations for bimolecular systems, such as limited electron transfer efficiency between dye and coinitiator or back electron transfer, can significantly decrease the initiation efficiency.[23] The rational design of unimolecular hydrophilic chromophores with high TPA activity can effectively overcome these drawbacks. In spite of foreseen advantages, true water-

DOI: 10.1039/C3RA42918K

soluble TPA PIs are still very rare.

Since a full understanding of the relationship of molecular structure and two-photon properties still remains a big challenge,[24] the most effective way to produce efficient water-soluble TPA PIs is to introduce water-borne functional groups, such as quaternary ammonium cations[6, 25] or carboxylic sodium salts,[26] onto the known core structures possessing high TPA initiation efficiency. One successful example of such rational molecular design is a distyrylbenzene chromophore with quaternary ammonium cations (**WSPI**) (Fig 1), which has proven to be a potent hydrophilic TPA PI and was used to fabricate 3D hydrogel scaffolds in the presence of a living organism.[27] Following the same strategy, Wu's group reported a benzylidene cyclopentanone dyes with hydrophilic sodium carboxylate group at the terminal alkyl chains.[22] They applied the molecule alone or used it as a sensitizer combined with triethanolamine for TPIP under aqueous condition. Our latest study on a series of hydrophobic benzylideneketone dyes shows that different sizes of the central rings have significant effect on their activity as initiators in TPIP.[28] Therefore, higher initiation efficiency would be expected while altering the central five-member ring as in **P2CK** to six-member ring as in **E2CK** (Fig 1). Additionally, the singlet oxygen quantum yields of chromophores bound to cyclohexanone are much lower than that of its cyclopetanone analogue.[29] Lower singlet oxygen quantum yields mean lower photoinduced cytotoxicity, which is critical for cell encapsulation. Besides studying the central ring effect, 4-methyl-cyclohexanone based initiators with different alky chain spacers as in **E2CK** and **G2CK** are of interest to investigate the structure-property relationship. Different lengths of alkyl chains at amino groups have previously proved to significantly affect the TPA at the desired wavelengths,[30] and therefore the initiation efficiency for polymerization.

In this paper, a series of benzylidene ketone-based water-soluble PIs with different size cycloketone rings were synthesized. Carboxylic acid salts were used as water-borne functionalities at the end of the amino moieties using alkyl chains as spacers. Two photon cross-section measurements via z-scan, as well as TPIP structuring tests were performed to evaluate the TPA properties of the initiators. Ideal structuring parameters for each initiator were determined by changing the laser intensity and the feed rate using the same molar PI concentrations. As the project aims to realize the fabrication of 3D hydrogel scaffolds in the presence of living cells, preliminary dark cytotoxicity tests of the TPA PIs were performed and the obtained results were compared to those of Irgacure 2959 (I2959) (Fig 1), the most commonly used photoinitiator in cell encapsulation.

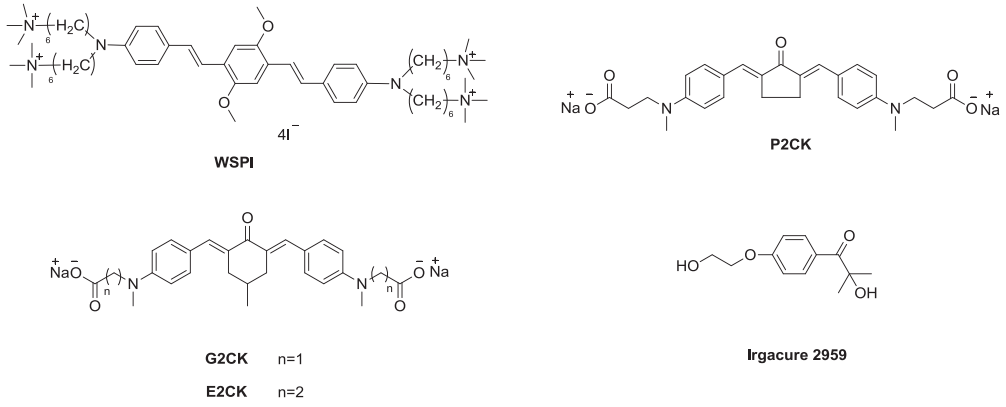

Fig. 1 Structures of TPA PIs and reference compounds

RESULTS AND DISCUSSION

Synthesis

Aldol condensation is a powerful tool for the synthesis of conjugated systems. Compared to other methods used in synthesizing TPA chromophores, such as Heck[31] and Sonogashira[32] coupling reactions, aldol condensation is more practical and economical.[28] Those features are particularly important for larger scale industrial preparations. Therefore, all novel water-soluble TPA PIs were synthesized via a classical aldol condensation reaction between 4-aminobenzaldehydes with carboxylic acid salts at terminal amino groups and corresponding ketones (Scheme 1).

Generally, one equivalent of the corresponding ketone was deprotonated at the α-position under alkaline conditions. Water was used as solvent due to the hydrophilicity of the aldehyde precursors. The formed enol was converted with two equivalents of the aldehyde and the products were precipitated by acidification. The final products with carboxylic acid salts were obtained after neutralization of the acids with dilute NaOH solution. Satisfying yields of 50 % were obtained for **P2CK**. By increasing the size of the central ring from cyclopentanone to 4-methylcyclohexanone, the yields decreased to 33% and 30% for **G2CK** and **E2CK**, respectively. Reduced yields may derive from sterical hindrance of the cyclohexanone ring, which is obstructive for the nucleophilic addition reaction. Such an effect was also observed for the synthesis of analogous hydrophobic cyclohexanones.[28]

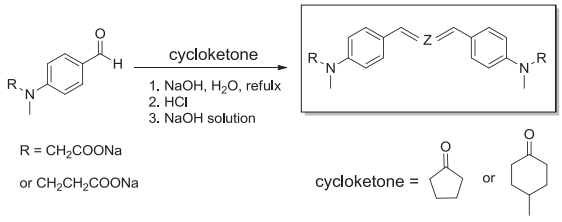

Scheme. 1 Reaction scheme for the synthesis of water-soluble TPA PIs

Cytotoxicity Test

To determine the influence of different PIs on cell viability, two different cell types were used. MG63 osteosarcoma cells and outgrowth endothelial cells (OEC) were exposed to PIs dissolved in PBS for 10 and 30 minutes. Only **G2CK** had a significant effect (p = 0.0411 (10 min); p = 0.0087 (30 min)) on the viability of MG63 cells while the effects of the other PIs were comparable to the control (Fig 2a). In addition to MG63, we analyzed the PIs using primary endothelial cells, which, in contrast to MG63 cells, show physiological behaviour when cultured *in vitro*. When increasing the incubation time from 10 min to 30 min, a significant drop of the viable cell number were observed with 4-methylcyclohexanone-based initiators **G2CK** (p = 0.022) and **E2CK** (p = 0.0022). The dark cytotoxicity of cyclopentanone-based initiator **P2CK** is as low as that of the reference I2959 for 10 min. When the incubation time was prolonged to 30 min, **P2CK** also reduced cell viability (p = 0.026), but to a much less degree than the other two TPA PIs (Fig 2b).

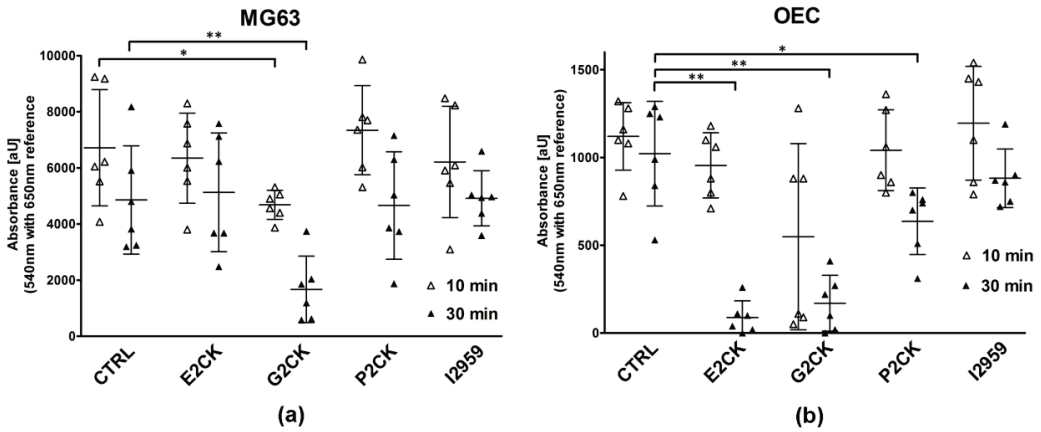

Fig. 2 Cytotoxicity of synthesized photoinitiators in two different cell types. (a) In MG63. (b) In OEC; aU: arbitrary units ; *p < 0.05 ; **p < 0.01

TPA Cross Section

To investigate the TPA properties of the new PIs, an open aperture z-scan analysis was performed to determine the TPA cross sections at 800 nm. Water was used as solvent for the TPA characterization of all the investigated PIs in Fig 3a as a representative example. In this figure, the full lines are the fitted curves using the adopted equations the adopted equations of Sheik-Bahae et al.[33] from which q_0 can be extracted for each pulse energy. To exclude excited-state absorption and to verify that a pure σ_{TPA} is determined, the measurements were repeated at different peak intensities For all samples it was verified that the calculated parameter q_0 scales linearly with intensity (Fig 3b). This proves that no excited-state absorption has occurred in the investigated samples. All calculated σ_{TPA} values are given in Table 1.

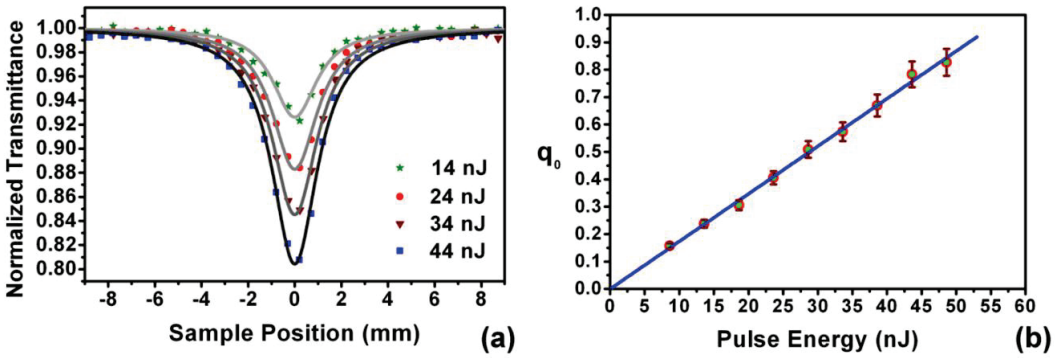

Fig. 3 (a) Experimental z-scan data (dots) and fitting curves (full lines) for **E2CK** at different pulse energies. (b) q_0 plotted vs. intensity for **E2CK** for standard measurement and fitting data.

The investigated TPA PIs comprise typical D-π-A-π-D core structures with C_{2v} symmetry, where alkylamino groups act as donors (D), vinyl as π-conjugated bridges and cycloketones as acceptors (A). Due to the long conjugation length and the presence of strong electron donor and acceptor groups, as well as good coplanarity derived from the cyclopentanone ring, the σ_{TPA} of **P2CK** is 176 GM at 800 nm in water. Such a value is substantially smaller than that of its hydrophobic analogue (466 GM in chloroform[28]). The reduction may be largely attributed to the solvent-effect on TPA behaviour. Various experimental and theoretical results demonstrated that TPA significantly depends on the surrounding medium and that the relation of TPA behaviour to solvent polarity may in fact be non-monotonic[34]. However, the σ_{TPA} of hydrophilic TPA

chromophores measured in water always drops considerably compared to that of their hydrophobic counterparts in organic solvents.[22] The exact mechanism still remains unclear at the present stage but the specific solute-solvent interactions such as hydrogen bonding or changes in the chromophore geometry and/or multichromophore aggregation are likely.[25]

When expanding the central ketone from cyclopetanone to 4-methylcyclohexanone as in **G2CK**, the σ_{TPA} value slightly dropped to 163 GM. The reduction in TPA absorption might be attributed to the non-planarity of the six-member ring, which leads to a decrease in the degree of conjugation. Interestingly, only a minor drop in σ_{TPA} of **G2CK** was observed compared to its hydrophobic counterpart with a σ_{TPA} of 191 GM.[28] It seems that the solvent-effect on TPA behaviour is not as significant for **G2CK** as for **P2CK**. One possibility is the sterical hindrance, derived from the non-planarity of the 4-methylcyclohexanone, which generally reduces aggregation. By extending the alkyl spacers from methylene to ethylene as in **E2CK**, the σ_{TPA} increased to 201 GM. This enhancement could derive from the stronger electron donating ability of amino groups with longer alkyl chains. Another reason might be the red-shift-induced large TPA absorption at the given wavelength.

As only the absorption behaviour could be obtained via z-scan measurement, TPIP structuring tests were performed to further assess TPA initiation efficiency of the new PIs.

Table 1. TPA cross section values (σ_{TPA}) of PIs in water by z-scan measurement at 800 nm

TPA PIs	σ_{TPA} (GM)
P2CK	176
G2CK	163
E2CK	201

TPIP Structuring Test

Several methods have been applied to evaluate the TPA initiation efficiency of initiators. The most popular one is single-line writing, in which the width of lines and threshold energies are used to quantify writing efficiency.[35] However, the method is not suitable here when considering the swelling property of hydrogels in water. Therefore, we use more complicated 3D shapes fabricated under various laser intensities and writing speeds to assess the efficiency. We find the method to be more practical since broad ideal processing windows are critical for high throughput in mass production and microfabrication of scaffolds with large size.[36] Defined lattices (lateral dimension: 50 × 50 μm, 10 μm hatch-distance, 5 μm layer-distance, 40 layers) were written into the hydrophilic formulation by means of TPIP to evaluate the activities of the PIs. A mixture of 50 wt% of polyetheleneglycol diacrylate (PEGda, 700 Da) and 50 wt% of DI water with the same PI concentration of 2 wt% was used. Good results had been previously obtained for such a formulation.[27]

In the experiments, the laser power was varied from 60 to 410 mW using increments of 50 mW for each element. Writing speed was adjusted from 1 to 100 mm/s. After fabrication and subsequent development, the whole structure array was visualized via focal laser scanning microscopy (LSM). (LSM images of all initiators with full processing windows are shown in the supporting information Fig S1). Different levels of fluorescence denote differences in the density of the polymer network.[27]

In order to qualitatively assess the TPA initiation efficiency of the initiators, three classes were employed to represent the quality of the structures (Fig 4). Class A (green area) defines excellent structures with well recognized straight lines and class B (yellow area) good structures with thick hatch-lines (compared to class A) or slightly contorted wavy lines. Structures rated as class C (red area) have identified shapes but with slight mistakes (e.g., holes, burst regions due to overexposure) or with thick lines growing together.

Both **E2CK** and **P2CK** contain a D-π-A-π-D core structure although the central cycloketone ring differs in size. The hydrophobic initiator with a benzylidenecyclohexanone core structure has recently been proven as a very efficient TPA PI in TPIP tests.[28] Via introduction of carboxylic sodium salts as hydrophilic moieties, the hydrophilic initiator **E2CK** also exhibits high initiation efficiency in photoactive formulation with 50 wt% of DI water. The threshold power of **E2CK** is 110 mW at a writing speed of 10 mm/s, which was found to be not sufficiently intense to trigger polymerization in a similar formulation containing the benzylidenecyclopentanone-based initiator **P2CK**. Such a trend is more significant as writing speed is increased: at the highest applied writing speed of 100 mm/s, the threshold energy is 210 mW for **E2CK**, whereas 100 mW of additional power is required when processing with **P2CK**. Besides lower threshold energies, the ideal processing windows (class A) of **E2CK** are larger than those of **P2CK**. One possible explanation for this enhancement is the larger TPA cross section of **E2CK** (201 GM) compared to that of **P2CK** (176 GM). Another more likely reason is the central ring effect, which significantly affects the fluorescence emission. Central cyclohexanone compounds possess much weaker fluorescence than their cyclopentanone counterparts.[37] Low fluorescence quantum yields are essential for efficient photoinitiators as they lead to less radiative deactivation and a higher population of the active state for initiating the polymerization.[32] The effect of ring geometry on initiation efficiency has recently been confirmed when studying the TPIP behaviour of several hydrophobic benzylidene ketones with different central rings.[28] In comparison to the five-member ring based initiator **P2CK**, the six-member ring analogue **E2CK** was also expected to show higher efficiency. Although **P2CK** offers smaller processing windows than **E2CK,** it is still substantially better performing than conventional xanthene dyes which exhibited at least 5 times smaller processing windows with the identical parameters (data not shown).

G2CK and **E2CK** share the same benzylidenecyclohexanone core structures but with different alkyl chain spacers. Although **E2CK** exhibits a larger σ_{TPA} than **G2CK**, the processing windows of the two PIs are very similar in TPIP tests. Since **G2CK** contains methyl-substituted phenylglycine moieties, which have been proven to be more active than other aromatic

amines as co-initiators in UV photopolymerization,[38] the enhanced performance of **G2CK** in TPIP might derive from the higher initiating efficiency of the formed radicals. Notably, when writing speed is increased above 20 mm/s, both **G2CK** and **E2CK** permit fabrication employing laser power as high as 410 mW without destruction of the microstructures. Good resistance to high laser power can also allow fast writing speed but with sufficient energy to induce polymerization. Delicate microstructures of hydrogels could be obtained even at a fabrication rate as high as 100 mm/s. To the best of our knowledge, it is the fastest writing speed up to now for 3D hydrogel microfabrication via TPIP. Enhanced writing speeds are critical for high throughput in mass production, especially when processing scaffolds with large size.

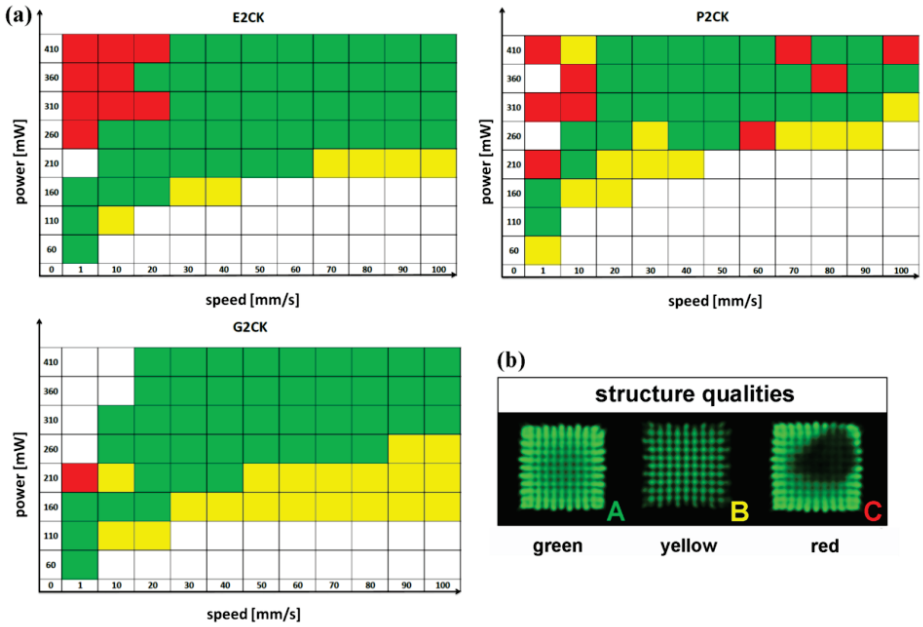

Fig. 4 (a) Processing windows of investigated initiators in TPIP screening tests; (b) Classification of the structures by the typical quality of their shapes.

With the same formulation containing **G2CK** as initiator, we structured 3D objects based on a CAD model (insert in Fig 5a) with intended dimensions of 200 × 170 × 94 μm^3. The array of fabricated hydrogel frogs along with a detailed view of an individual frog object is shown in Fig 4. High spatial resolution combined with complex 3D structures with massive overhangs, which are otherwise inaccessible for other fabrication techniques, could be easily obtained.

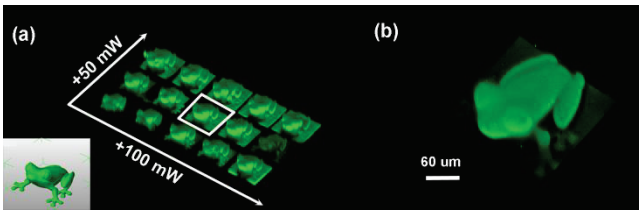

Fig. 5 Fabrication of a CAD frog in a 1:1 PEGda: DI water hydrogel formulation containing 2 wt% of G2CK using a 20× NA 0.8 objective, (a) Fabricated array at 15 mm/s with different laser powers (100-240 mW), stacked 3D LSM image, insert is the CAD model; (b) Detailed view of the LSM image of the white marked structure.

EXPERIMENTAL

Materials

All reagents for synthesis were purchased from Sigma-Aldrich, Fluka, and ABCR and were used without further purification. The solvents were dried and purified by standard laboratory methods. Column chromatography was performed with conventional techniques on VWR silica gel 60 (0.040-0.063 mm particle size). Aluminum-backed silica gel plates were used for TLC analyses.

Synthesis

Detailed synthetic procedure of precursors for condensation reactions are given in the Supporting Information.

General procedure for aldol condensation reaction

In an orange light room, 0.25 mmol of sodium hydroxide, 4.52 mmol of the benzaldehyde compound and 2.26 mmol of freshly distilled cycloketone compound were dissolved in 10 mL of water. The reaction was stirred at 80 °C for 4h and then cooled to room temperature. 20 mL of EtOH and 1M HCl were added consequently until no precipitate formed. The red solids were collected by centrifugation and dried in vacuum. The obtained solids were put into 20 mL of water and 0.1M NaOH was added dropwise until pH 8.5 was reached (monitored with pH meter). The undissolved solids were filtered off and water was removed via freeze-drying to yield desired products.

Sodium 3,3'-((((1E,1'E)-(2-oxocyclopentane-1,3-diylidene) bis (methanylylidene))bis(4,1-phenylene))bis(methylazanediyl)) dipropanoate (**P2CK**)

Orange powder with a yield of 50%. Mp: >300 °C. ^{1}H NMR (200MHz, D_2O) δ = 7.10 (d, J = 8.2 Hz, 4 H), 6.94 (s, 2 H), 6.40

(d, J = 8.2 Hz, 4 H), 3.39 (t, J = 7.1 Hz, 4 H), 2.49 - 2.42 (m, 4 H), 2.24 (t, J = 7.2 Hz, 4 H). ^{13}C NMR (50MHz, D_2O) δ = 196.9, 180.7, 149.7, 135.0, 133.3, 132.7, 123.1, 111.9, 49.1, 37.3, 34.7, 26.4. Anal. Calcd for $C_{27}H_{28}N_2O_5Na_2$: C, 64.03; H, 5.57; N, 5.53; Found: C, 64.33; H, 5.38; N, 5.42.

Sodium 3,3'-((((1E,1'E)-(5-methyl-2-oxocyclohexane-1,3-diylidene)bis(methanylylidene))bis(4,1-phenylene))bis (methylazanediyl)) dipropanoate (**E2CK**)

Orange powder with a yield of 30%. Mp: >300 °C. ^{1}H NMR (200MHz, D_2O) δ = 7.40 (s, 2 H), 7.27 (d, J = 8.6 Hz, 4 H), 6.63 (d, J = 8.6 Hz, 4 H), 3.49 (t, J = 7.1 Hz, 4 H), 2.78 (s, 6 H), 2.73 - 2.67 (m, 2 H), 2.28 (t, J = 7.2 Hz, 4 H), 2.18 - 1.90 (m, 3 H), 0.83 (d, J = 6.3 Hz, 3 H). ^{13}C NMR (50MHz, D_2O) δ = 192.7, 181.1, 149.6, 138.7, 133.2, 131.5, 123.5, 112.2, 49.3, 37.4, 34.4, 20.7. Anal. Calcd for $C_{29}H_{32}N_2O_5Na_2$: C, 65.16; H, 6.03; N, 5.24; Found: C, 65.37; H, 5.92; N, 5.08.

Sodium 2,2'-((((1E,1'E)-(5-methyl-2-oxocyclohexane-1,3-diylidene) bis (methanylylidene)) bis(4,1-phenylene))bis (methylazanediyl))diacetate (**G2CK**)

Orange powder with a yield of 33%. Mp: >300 °C. ^{1}H NMR (200MHz, D_2O) δ = 7.44 (s, 2 H), 7.29 (d, J = 8.6 Hz, 4 H), 6.52 (d, J = 8.6 Hz, 4 H), 3.75 (s, 4 H), 2.88 (s, 6 H), 2.78 - 2.45 (m, 2 H), 2.23 - 1.94 (m, 3 H), 0.83 (d, J = 6.3 Hz, 3 H). ^{13}C NMR (50MHz, D_2O) δ = 192.6, 178.4, 150.2, 138.9, 133.2, 131.2, 123.0, 111.4, 56.1, 28.6, 20.9. Anal. Calcd for $C_{27}H_{28}N_2O_5Na_2$: C, 64.03; H, 5.57; N, 5.53; Found: C, 64.31; H, 5.33; N, 5.47.

Characterization

^{1}H NMR (200 MHz) and ^{13}C NMR (50 MHz) spectra were measured with a BRUKER ACE 200 FT-NMR-spectrometer. The chemical shift (s = singlet, bs = broad singlet, d = doublet, t = triplet, m = multiplet) is stated in ppm using the nondeuterated solvent as internal standard. Solvents with a grade of deuteration of at least 99.5% were used. Melting points were measured on a Zeiss axioscope microscope with a Leitz heating block and remained uncorrected. GC-MS runs were performed on a Thermo Scientific DSQ II using a BGB 5 column (l = 30 m, d = 0.32 mm, 1.0 µm film; achiral). Elemental microanalysis was carried out with an EA 1108 CHNS-O analyzer from Carlo Erba at the microanalytical laboratory of the Institute for Physical Chemistry at the University of Vienna.

Cell culture and MTT assay

Outgrowth endothelial cells (OECs) were isolated from two different donors as described elsewhere.[39, 40] All donors gave written formal consent to the use of the biological material, with formal approval by the local ethical committee. OECs were cultured in full EGM-2 medium (Lonza) containing 5% FBS on plastic dishes coated with 2 µg mL^{-1} fibronectin (Sigma). The cells were used between passages 5 and 9 for cytotoxicity experiments. The osteosarcoma cell line MG63 was cultured in DMEM containing 10% FBS. To determine the cytotoxicity of different photoinitiators, 10^4 cells were seeded in selected wells on a 96-well plate (Corning) and incubated over night at 37°C. Photoinitiators were dissolved in 1× PBS without Ca^{2+} and Mg^{2+} to a final concentration of 1.82 mM. Before exposing the cells to the PI solution, the supernatants were aspirated and the cells were washed once with PBS. The sterile-filtered PI solution was added to the cells and the plate was incubated for 10 or 30 minutes at 37 °C. The PI solution was removed and cells were washed twice with PBS. Fresh growth medium was then added to the cells. All steps were performed without direct exposure to light. Following additional 24 hours of incubation, the supernatants were removed and cells were washed three times with PBS. MTT reagent (Sigma) was dissolved in 1× PBS (5 g/L). Before adding to the cells, this stock solution was diluted with the respective growth medium to 3.25 g/L and the plate was incubated for 1 hour at 37°C. The supernatant was removed and formazan crystals were dissolved using dimethyl sulfoxide (Sigma). The plate was incubated on a shaker in the dark at room temperature for 20 minutes and absorbance was measured at 540 nm with 650 nm as reference.

Raw data were collected from two different experiments done in triplicate and analyzed using Prism 5 (Graphpad). Significance was determined using nonparametric, unpaired, two-tailed Mann-Whitney test (each PI group vs. control group).

Z-scan analysis

A Ti: sapphire laser system (90 fs pulse duration, 1 kHz repetition rate) was used for the open aperture z-scan analysis. A detailed description of the setup and the fitting equations used can be found elsewhere.[32] Rhodamine B in MeOH was used as reference to verify the reliability of the experimental setup. All PIs were prepared as 1.0 × 10^{-2} M solutions in spectroscopic grade water. The PI solutions were measured in a 0.2 mm thick flow cell in a non-recycling volumetric flow of 4 mL/h. The excited volume is therefore refreshed approximately every 100 pulses, which approximately corresponds to 10 times for each z-position, which was found to be sufficient. The measurements were carried out at different pulse energies in the range of 14-240 nJ. At higher energies a signal of the pure solvent appears and the solvent will contribute to the effective nonlinear absorption and even thermal effects are more likely to influence the measurement. Care had to be taken to collect the whole transmitted laser energy using a big diameter and short focal length lens. Additionally, a proper Gaussian beam profile in time and space is essential for the analysis.

TPIP Structuring Tests

Laser Device

For the direct laser writing of 3D structures, a Ti: sapphire laser providing NIR pulses at 780 nm wavelength with a pulse duration of 100 fs is used. The system operates at a repetition rate of 80 MHz. the laser power ranged from 60 to 410 mW (measured before passing a 20× NA 0.8 microscope objective). The increment was set to 50 mW with each element. The writing speed was adjusted from 1 to 100 mm/s at increments of 10 mm/s.

General Procedure

For all samples the same fabrication process was implemented: The optical material was drop-cast onto a glass substrate, which had been functionalized with methacrylate functional groups according to literature.[41] Subsequently, the samples were exposed to the laser beam, and the focus was scanned across the photosensitive material, which leads to an embedded 3D structure inside the material volume. After laser writing, the unexposed material was removed by development of the structure in ethanol (rinsing). The resulting array structures could be visualized via LSM.

Conclusions

A series of benzylidene ketone-based hydrophilic two-photon initiators, containing carboxylic acid sodium salts for improved water-solubility, dialkylamino groups as donors and double bonds as conjugation bridges, were efficiently synthesized via classical aldol condensation reactions. The dark cytotoxicity of 4-methylcyclohexanone-based initiators significantly increased with increasing incubation time, especially for OEC. The cyclopentanone-based initiator yields the highest cytocompatibility comparable to Irgacure 2959 for both MG63 and OEC. Due to the long conjugation length and the presence of strong electron donors and acceptors, the investigated water-soluble TPA PIs exhibited moderate TPA cross sections ranging from 163 GM to 201 GM at 800 nm in water. The TPA cross section values obtained under aqueous condition are reduced compared to those of their hydrophobic analogues measured in organic solvents. In TPIP tests using various laser powers and writing speeds, all novel initiators exhibited large ideal processing windows for hydrophilic photopolymers with up to 50 wt% of water. The ideal processing windows of the cyclohexanone initiators (**G2CK** and **E2CK**) are broader than those of cyclopentanone initiators such as **P2CK**. Impressively, a writing speed as high as 100 mm/s was obtained for precise microfabrication of hydrogels.

The authors acknowledge the financial support by the China Scholarship Council (CSC, no. 2009688004), Austrian Science Fund (FWF), the European Commission under contracts 260043 (PHOCAM) and 262027 (LebMEC), and the European Science Foundation (ESF) with P2M network. Thanks also to Dr. S.C. Ligon for grammatical revisions.

Notes and references

[a] *Institute of Applied Synthetic Chemistry, Vienna University of Technology, Getreidemarkt 9/163/MC, 1060 Vienna, Austria, E-mail: robert.liska@tuwien.ac.at*
[b] *Institute of Materials Science and Technology, Vienna University of Technology, Favoritenstrasse. 9-11, 1040 Vienna, Austria*
[c] *Institute of Applied Physics, Vienna University of Technology Wiedner Hauptstrasse 8, 1060 Vienna, Austria*
[d] *Ludwig Boltzmann Institute for Experimental and Clinical Traumatology, Donaueschingenstrasse, 13, 1200 Vienna, Austria*
[e] *Austrian Cluster for Tissue Regeneration, Donaueschingenstrasse, 13, 1200 Vienna, Austria*

† Electronic Supplementary Information (ESI) available: synthesis of the precursors and processing windows of TPA PIs. See DOI: 10.1039/b000000x/

1. G. Justin, S. Finley, A. Abdur Rahman and A. Guiseppi-Elie, *Biomed. Microdevices*, 2009, **11**, 103.
2. A. Ovsianikov, V. Mironov, J. r. Stampf and R. Liska, *Expert. Rev. Med. Devic*, 2012, **9**, 613.
3. T. Billiet, M. Vandenhaute, J. Schelfhout, S. Van Vlierberghe and P. Dubruel, *Biomaterials*, 2012, **33**, 6020.
4. B. H. Cumpston, S. P. Ananthavel, S. Barlow, D. L. Dyer, J. E. Ehrlich, L. L. Erskine, A. A. Heikal, S. M. Kuebler, I. Y. S. Lee, D. McCord-Maughon, J. Qin, H. ckel, M. Rumi, X.-L. Wu, S. R. Marder and J. W. Perry, *Nature*, 1999, **398**, 51.
5. S. Maruo, O. Nakamura and S. Kawata, *Opt Lett*, 1997, **22**, 132.
6. X. Shen, L. Li, A. C. Min Chan, N. Gao, S. Q. Yao and Q.-H. Xu, *Adv. Opt. Mater*, 2013, **1**, 92.
7. M. S. Hahn, J. S. Miller and J. L. West, *Adv. Mater*, 2005, **17**, 2939.
8. R. Schade, T. Weiss, A. Berg, M. Schnabelrauch and K. Liefeith, *Int. J. Artif. Organs,* 2010, **33**, 219.
9. A. Ovsianikov, M. Gruene, M. Pflaum, L. Koch, F. Maiorana, M. Wilhelmi, A. Haverich and B. Chichkov, *Biofabrication*, 2010, **2**, 014104/014101.
10. S. Li, L. Li, F. Wu and E. Wang, *J. Photoch. Photobio. A*, 2009, **203**, 211.
11. S. J. Jhaveri, J. D. McMullen, R. Sijbesma, L.-S. Tan, W. Zipfel and C. K. Ober, *Chem. Mater*, 2009, **21**, 2003.
12. G. Wang, K.-Y. Pu, X. Zhang, K. Li, L. Wang, L. Cai, D. Ding, Y.-H. Lai and B. Liu, *Chem. Mater*, 2011, **23**, 4428.
13. X. Wang, D. M. Nguyen, C. O. Yanez, L. Rodriguez, H.-Y. Ahn, M. V. Bondar and K. D. Belfield, *J. Am. Chem. Soc*, 2010, **132**, 12237.
14. M. Taki, J. L. Wolford and T. V. O'Halloran, *J. Am. Chem. Soc*, 2004, **126**, 712.
15. M. A. Albota, C. Xu and W. W. Webb, *Appl. Optics*, 1998, **37**, 7352.
16. A. Ovsianikov, A. Deiwick, S. Van Vlierberghe, M. Pflaum, M. Wilhelmi, P. Dubruel and B. Chichkov, *Materials*, 2011, **4**, 288.
17. A. Vogel and V. Venugopalan, *Chem Rev*, 2003, **103**, 577.
18. P. J. Campagnola, D. M. Delguidice, G. a. Epling, K. D. Hoffacker, A. R. Howell, J. D. Pitts and S. L. Goodman, *Macromolecules*, 2000, **33**, 1511.
19. M. Farsari, G. Filippidis, K. Sambani, T. S. Drakakis and C. Fotakis, *J. Photoch. Photobio. A* 2006, **181**, 132.
20. J. D. Pitts, P. J. Campagnola, G. a. Epling and S. L. Goodman, *Macromolecules*, 2000, **33**, 1514.
21. S. Basu, V. Rodionov, M. Terasaki and P. J. Campagnola, *Opt. Lett*, 2005, **30**, 159.
22. X. Wan, Y. Zhao, J. Xue, F. Wu and X. Fang, *J. Photoch. Photobio. A*, 2009, **202**, 74.
23. G. Ullrich, P. Burtscher, U. Salz, N. Moszner and R. Liska, *J. Polym. Sci. Pol. Chem*, 2006, **44**, 115.
24. N. Pucher, A. Rosspeintner, V. Satzinger, V. Schmidt, G. Gescheidt, J. r. Stampfl and R. Liska, *Macromolecules*, 2009, **42**, 6519.
25. H. Y. Woo, B. Liu and B. Kohler, *J. Am. Chem. Soc*, 2005, **127**, 14721.
26. C. Cepraga, T. Gallavardin, S. Marotte, P.-H. Lanoe, J.-C. Mulatier, F. Lerouge, S. Parola, M. Lindgren, P. L. Baldeck, J. Marvel, O. Maury, C. Monnereau, A. Favier, C. Andraud, Y. Leverrier and M.-T. Charreyre, *Polym. Chem*, 2013, **4**, 61.

27. J. Torgersen, A. Ovsianikov, V. Mironov, N. Pucher, X. Qin, Z. Li, K. Cicha, T. Machacek, R. Liska, V. Jantsch and J. Stampfl, *J. Biomed. Opt* 2012, **17**, 105008.
28. Z. Li, N. Pucher, K. Cicha, J. Torgersen, S. C. Ligon, A. Ajami, W. Husinsky, A. Rosspeintner, E. Vauthey, S. Naumov, T. Scherzer, J. r. Stampfl and R. Liska, *Macromolecules*, 2013, **46**, 352.
29. Q. Zou, Y. Zhao, N. S. Makarov, J. Campo, H. Yuan, D.-C. Fang, J. W. Perry and F. Wu, *Phys Chem Chem Phys*, 2012, **14**, 11743.
30. N. Pucher, A. Rosspeintner, V. Satzinger, V. Schmidt, G. Gescheidt, J. r. Stampfl and R. Liska, *Macromolecules*, 2009, **42**, 6519.
31. T.-C. Lin, C.-S. Hsu, C.-L. Hu, Y.-F. Chen and W.-J. Huang, *Tetrahedron Lett*, 2009, **50**, 182.
32. Z. Li, M. Siklos, N. Pucher, K. Cicha, A. Ajami, W. Husinsky, A. Rosspeintner, E. Vauthey, G. Gescheidt, J. Stampfl and R. Liska, *J Polym Sci Pol Chem*, 2011, **49**, 3688.
33. M. Sheik-bahae, A. A. Said, T. H. Wei, Y. Y. Wu, D. J. Hagan, M. J. Soileau and S. E. W. Van, *Proc. SPIE-Int. Soc. Opt. Eng.*, 1990, **1148**, 41.
34. A. Nag and D. Goswami, *J Photoch Photobio A*, 2009, **206**, 188.
35. J.-F. Xing, X.-Z. Dong, W.-Q. Chen, X.-M. Duan, N. Takeyasu, T. Tanaka and S. Kawata, *Appl. Phys. Lett*, 2007, **90**, 131106/131101.
36. K. Cicha, Z. Q. Li, K. Stadlmann, A. Ovsianikov, R. Markut-Kohl, R. Liska and J. Stampfl, *J. Appl. Phys*, 2011, **110**, 064911.
37. K. Yamashita, S. Imahashi and S. Ito, *Dyes. Pigments*, 2007, **76**, 748.
38. J. Lalevee, B. Graff, X. Allonas and J.-P. Fouassier, *J. Phys. Chem. A*, 2007, **111**, 6991.
39. S. Fuchs, M. I. Hermanns and C. J. Kirkpatrick, *Cell. Tissue. Res*, 2006, **326**, 79.
40. W. Holnthoner, K. Hohenegger, A.-M. Husa, S. Muehleder, A. Meinl, A. Peterbauer-Scherb and H. Redl, *J. Tissue. Eng. Regen. M,* 2012.
41. C. A. Goss, D. H. Charych and M. Majda, *Anal. Chem*, 1991, **63**, 85.